

Copyright © 1992, by the author(s).
All rights reserved.

Permission to make digital or hard copies of all or part of this work for personal or classroom use is granted without fee provided that copies are not made or distributed for profit or commercial advantage and that copies bear this notice and the full citation on the first page. To copy otherwise, to republish, to post on servers or to redistribute to lists, requires prior specific permission.

**NEW TYPE OF STRANGE ATTRACTOR
RELATED TO THE CHUA'S CIRCUIT**

by

V. N. Belykh and L. O. Chua

Memorandum No. UCB/ERL M92/52

15 April 1992

COVER PAGE

**NEW TYPE OF STRANGE ATTRACTOR
RELATED TO THE CHUA'S CIRCUIT**

by

V. N. Belykh and L. O. Chua

Memorandum No. UCB/ERL M92/52

15 April 1992

ELECTRONICS RESEARCH LABORATORY

College of Engineering
University of California, Berkeley
94720

TITLE PAGE

This work is supported in part by the Office of Naval Research under grant N00014-89-J-1402 and the National Science Foundation under grant MIP-8912639.

**NEW TYPE OF STRANGE ATTRACTOR
RELATED TO THE CHUA'S CIRCUIT**

by

V. N. Belykh and L. O. Chua

Memorandum No. UCB/ERL M92/52

15 April 1992

ELECTRONICS RESEARCH LABORATORY

College of Engineering
University of California, Berkeley
94720

This work is supported in part by the Office of Naval Research under grant N00014-89-J-1402 and the National Science Foundation under grant MIP-8912639.

NEW TYPE OF STRANGE ATTRACTOR RELATED TO THE CHUA'S CIRCUIT

V.N.Belykh

Mathematics department
N.Novgorod Institute of Water-Transport Engineers
603600 N.Novgorod, Russia

L.O.Chua

Department of Electrical Engineering and Computer Sciences
University of California, Berkeley, CA 94720, USA

We present a new type of strange attractors generated by an odd-symmetric 3-dimensional vector field with a saddle-focus having two homoclinic orbits at the origin. This type of attractors is intimately related to the double scroll. We present the mathematical properties which proved rigorously the chaotic nature of this strange attractor to be different from that of a Lorenz-type attractor or a quasi-attractor.

In particular, we proved that for certain non-empty intervals of parameters, our 2-dimensional map has a strange attractor *with no stable orbits*. Unlike other known attractors, this strange attractor contains not only a Cantor set structure of hyperbolic points typical of horseshoe maps, but also there exists *unstable points* (i.e., stable in reverse time) belonging to the attractor as well. This implies that the points from the stable manifolds of the hyperbolic points must necessarily attract the unstable points.

1. Geometric Model

Consider the class of 3-dimensional piecewise-linear system (PL-system) satisfying the following conditions.

1) Inside the cylinder (see Fig.1)

$$G = \{ |x| \leq h, y^2 + z^2 \leq r^2 \}$$

The PL-system is defined by the following linear system in the normal form

$$\dot{x} = \gamma x, \quad \dot{y} = -\sigma y - \omega_0 z, \quad \dot{z} = \omega_0 y - \sigma z \quad (1.1)$$

To avoid repetition, and to exploit the odd-symmetry of our geometric model, where many items occur in pairs, we will use a "parenthesis" to denote the corresponding symmetrical statement, symbol, concept, components of the cylinder surface, etc. Hence, the boundary ∂G of the cylinder G will be denoted by

$$\partial G = \bigcup_i D_i \cup d_h^i, \quad i=1,2$$

where

$$D_{1(2)} = \{ y^2 + z^2 = r^2: 0 < x \leq h \text{ (} 0 > x \geq -h \text{)} \}$$

denotes the upper (lower) cylinder bounding surface, except the common boundary at $x=0$,

$$d_h^{1(2)} = \{ y^2 + z^2 \leq r^2: x=h \text{ (} x=-h \text{)} \}$$

denotes the top and bottom disks, and

$$D = D_1 \cup D_2 \cup \{ y^2 + z^2 = r^2: x=0 \}$$

denotes the cylinder boundary surface.

2) Outside of the cylinder G , the PL-system generates an odd-symmetric linear Poincare map S such that $S|_{d_h^{1(2)}} = S_{1(2)}: d_h^{1(2)} \rightarrow D$. The two points $(\pm h, 0, 0)$ lying on the 1-dimensional unstable manifold Γ_1 (Γ_2) of (1.1) have the images $P_{1(2)} = S_{1(2)}(\pm h, 0, 0) \subset D$. These two points are shown in Fig.1 for the case when the x -coordinate is zero. Hence, the global unstable manifold Γ_1 (Γ_2) of the PL-system returns to ∂G , i.e. $P_{1(2)} = \Gamma_{1(2)} \cap D$.

Some typical trajectories of the PL-system which are homeomorphic to corresponding trajectories from Chua's circuit [Matsumoto, 1984, Chua et.al., 1986, Komuro et.al., 1991] are shown in Fig.1.

Let us define T [Shil'nikov, 1965] which maps the PL-system trajectories

inside G , originating from the cylinder surfaces $D_{1(2)}$ into the top and bottom disks $d_h^{1(2)}$; namely $T|_{D_{1(2)}} = T_{1(2)}: D_{1(2)} \rightarrow d_h^{1(2)}$. Hence, the global Poincare map is given by $f=ST$, where $f|_{D_{1(2)}} = f_{1(2)} = S_{1(2)}T_{1(2)}: D_{1(2)} \rightarrow D$.

Using the polar coordinates

$$y = \rho \cos \phi, \quad z = \rho \sin \phi \quad (1.2)$$

and solving the Shil'nikov's boundary problem (trivial in our case) we obtain the following formulas for the mapping $T: (\phi(0), x(0)) \rightarrow (y(\tau), z(\tau))$:

$$\begin{aligned} y(\tau) &= \rho(\tau) \cos \phi(\tau), \quad z(\tau) = \rho(\tau) \sin \phi(\tau), \\ \rho(\tau) &= a_1 |x(0)|^\nu, \quad \phi(\tau) = \phi(0) + \phi_1 - \omega \ln |x(0)|, \\ \nu &= \sigma/\gamma, \quad \omega = \omega_0/\gamma, \quad a_1 = rh^{-\nu}, \quad \phi_1 = \omega \ln h. \end{aligned} \quad (1.3)$$

where $\tau = \gamma^{-1} \ln h |x(0)|^{-1}$ is the elapse time of motion from the cylinder surface D to the top (bottom) disk $d_h^{1(2)}$ along the trajectories of (1.1).

Consider the following simplest linear mapping $S: (y, z) \in d_h^{1(2)} \rightarrow (\phi, x) \in D$ which realizes the global picture of the PL-system shown in Fig.1:

$$\begin{aligned} S_i U &= S_{0i} + S_{1i} U, \quad i=1,2, \\ U &= \begin{pmatrix} u_1 \\ u_2 \end{pmatrix}, \quad S_{0i} = \begin{pmatrix} (1-i)\pi + \psi \\ (-1)^{i+1} \mu \end{pmatrix}, \quad S_{1i} = \begin{pmatrix} (-1)^i \alpha \sin \theta & (-1)^{i+1} \alpha \cos \theta \\ \alpha \cos \theta & \alpha \sin \theta \end{pmatrix} \end{aligned} \quad (1.4)$$

Here, (u_1, u_2) denotes the coordinates (y, z) of the initial point on the top or

bottom disc, S_{0i} denotes the coordinate vector of the return points P_i , $i=1,2$, where, the x and ϕ coordinates of the return point are translated by two constant parameters μ and ψ for the sake of generality, θ denotes the torsion angle of the twisting of the disks $d_{1(2)}$ as it maps into D , α^2 denotes the contraction (expansion) coefficient of the linear maps S , and the signs of the $\det S_{1i}$ are chosen to match the orientation of the coordinates $\{y,z\}$ and $\{\phi,x\}$. Substituting $(y(\tau),z(\tau))$ from (1.3) for (u_1,u_2) in (1.4), we obtain the following explicit formulas for the discontinuous map f of the PL-system:

$$\begin{aligned}\bar{\phi} &= -\frac{\pi}{2} + \left(\frac{\pi}{2} + a|x|^V \cos(\phi + \varphi - \omega \ln|x|)\right) \text{sgn } x, \quad x \neq 0, \quad x \in D \\ \bar{x} &= \mu \text{sgn } x - a|x|^V \sin(\phi + \varphi - \omega \ln|x|), \quad x \neq 0, \quad x \in D,\end{aligned}\tag{1.5}$$

where $\text{sgn}(\cdot)$ denotes the signum function, and where

$$\begin{aligned}\varphi &\triangleq \psi + \phi_1 - \theta - \pi/2, \quad a \triangleq \alpha a_1, \\ \phi &\triangleq \phi(0) - \psi, \quad x \triangleq x(0), \quad \bar{\phi} \triangleq \phi(\tau) - \psi, \quad \bar{x} \triangleq x(\tau)\end{aligned}\tag{1.6}$$

Observe that $f(\cdot)$ is discontinuous at $x=0$ because any point located at an infinitesimal distance above $x=0$ must map into a neighborhood of P_1 , whereas, any point located below $x=0$ must map into a neighborhood of P_2 . Observe also that $f(\cdot)$ in (1.5) is undefined at $x=0$. However, in view of the above discontinuous behavior, we can define $f(x)$ at $x=0$ as follow:

$$\lim_{x \rightarrow 0 \downarrow} (\bar{\phi}, \bar{x}) \triangleq (0, \mu), \quad \lim_{x \rightarrow 0 \uparrow} (\bar{\phi}, \bar{x}) \triangleq (-\pi, -\mu).\tag{1.7}$$

Note that whereas v and ω are "local" parameters of (1.1), μ , a , and ϕ are "global" parameters: μ controls the return points $P_1(0,\mu)$ and $P_2(-\pi,-\mu)$, a is usually called the separatrix value and ϕ is the phase shift.

2. The images of the map f .

For simplicity and without loss of generality, let us assume that all parameters in (1.5) are nonnegative. It follows from (1.5) that for any $x=\text{const}$, $\phi \in S^1$, where S^1 denotes a topological circle, the image $(\bar{\phi}, \bar{x})$ is also a circle, and for any $\phi=\text{const}$, $|x| \leq h$, the image $(\bar{\phi}, \bar{x})$ is a spiral. Therefore, denoting the circles by $C_\eta^{1(2)} = \{x=\eta(-\eta), \phi \in S^1\}$, $\eta \geq 0$, and, the lines by $I_\xi^{1(2)} = \{\phi=\xi, 0 \leq x \leq \eta \ (-\eta \leq x \leq 0)\}$, at D we have:

Lemma 1. 1) The images $f_{1(2)} C_\eta^{1(2)}$ are circles defined, respectively by

$$\bar{\phi}^2 + (\bar{x} - \mu)^2 = a^2 \eta^{2v} \quad \text{and} \quad (\bar{\phi} + \pi)^2 + (\bar{x} + \mu)^2 = a^2 \eta^{2v} \quad (2.1)$$

2) The images $f_{1(2)} I_\xi^{1(2)}$ are "shrinking" spirals connecting the circle $f_1 C_\eta^1$ to the point P_1 , where it rotates in a clockwise direction as $|x|$ decreases ($f_2 C_\eta^1$ to the point P_2 where it rotates in a counter-clockwise directions as $|x|$ decreases, respectively) (see Fig.2).

Consider the one-to-one 1-D map $g: \mathbb{R}^1 \rightarrow \mathbb{R}^1$

$$\bar{x} = \mu + ax^v, \quad (2.2)$$

where $v < 1$, $a > 0$, $\mu > 0$.

Note, that $g(\cdot)$ is a contraction for $0 < x < x_1 = (\nu a)^{1/(1-\nu)}$, and an expansion for $x > x_1$.

Observe that g has a unique stable fixed point at $x=x_s$, $x_s > x_1 > \mu$ in view of the inequality $g' \Big|_{x=x_s} = v(1 - \frac{\mu}{x_s}) < 1$. Let us denote $D_\eta = \{ |x| \leq \eta \leq h, \phi \in S^1 \}$.

Lemma 2. Assume that the parameters in (1.5) satisfy the condition

$$v < 1, \quad a^{1/(1-v)} < h, \quad 0 \leq \mu \leq h - ah^v \quad (2.3)$$

Then

$$1) \quad fD \subset D \quad (f_{1(2)} D_{1(2)} \stackrel{\Delta}{=} \tilde{d}_{1(2)} \subset D).$$

2) There exist domains $d_i = f_i D_{x_s}$ defined by

$$d_i = \left\{ (x + (-1)^i \mu)^2 + (\phi - (1-i)\pi)^2 \leq a^2 x_s^{2v} \right\}, \quad i=1,2,$$

such that $fD_\eta \supset (d_1 \cup d_2)$ for $\eta > x_s$ and $fD_\eta \subset (d_1 \cup d_2)$ for $\eta < x_s$.

Proof. Denoting $\bar{\eta}$ as the maximum value of x for the image fD_η we immediately obtain the map $\bar{\eta} = g(\eta)$ defined by (2.2). Then the first assertion follows from $h < g(h)$ because of (2.3), and the second assertion is related to the fixed point $x_s = g(x_s)$.

Corollary. 1) The mapping f has an attractor

$$A = \lim_{P \rightarrow \infty} f^P D \subset (d_1 \cup d_2) \quad (2.4)$$

2) The domain $d_1 \cup d_2$ is the minimum attracting domain.

Hence in the following we consider $D = D_{x_s}$ ($h = x_s$) such that $d_i = f_i D_{x_s}$, $i=1,2$. Note that (1.5) implies the images of any set X are given by

$$f_i X = f_i (X \cap D_i), \quad i=1, 2$$

$$fX = f_1 (X \cap D_1) \cup f_2 (X \cap D_2) \quad (2.5)$$

Consequently the limit in (2.4) is to be interpreted in the sense of (2.5).

Let $\mu < ax_s^y$, then $d_i \cap C_0^1 \neq \emptyset$ Consider next the images

$$d_{ij} \triangleq f_j d_i, \quad i, j=1,2 \quad (2.6)$$

Due to (2.5) $d_{ij} = f_j f_i D = f_i (D_i \cap f_j D)$. By virtue of Lemma 1 d_{ij} has a snake-like spiral shape, henceforth called *S*-snakes (Shil'nikov's snakes) (see Fig.3).

The following assertion is a direct consequence of lemmas 1 and 2.

Lemma 3. 1) The *S*-snakes $d_{11}, d_{12} \subset d_1$ ($d_{22}, d_{21} \subset d_2$) rotate in a clockwise (counterclockwise) direction as $|x|$ decreases.

2) For $\mu > 0$ the *S*-snakes d_{ii} start at the points $M_{ii} = f_i M_i$, $i=1,2$, such that $M_1(0, x_s)$ ($M_2(-\pi, -x_s)$) and $M_{11}(M_{22})$ lie at the boundary of d_1 (d_2) and end at the points P_i , $i=1,2$, as $|x|$ decreases to zero. For $\mu=0$ all four *S*-snakes start at the corresponding boundaries of d_1 and d_2 .

3) $Rd_{22} = d_{11}$, $Rd_{21} = d_{12}$ where R denotes the inverse mapping $R: (\phi, x) \rightarrow (\phi + \pi, -x)$.

3. Preimages and *B*-operator.

Since f is a discontinuous map, the inverse map must be defined.

Definition 1. The inverse map f^{-1} is the map satisfying the following condition: for any set $X_i \subset D_i$ and $\bar{X}_i = f_i X_i$ then $f_i^{-1} \bar{X}_i = X_i$, $i=1,2$, independently of whether $\bar{X}_1 \cap D_2 = \emptyset$ and $\bar{X}_2 \cap D_1 = \emptyset$, or not.

It follows from (2.5) that if $X \cap D_i \neq \emptyset$, $i=1,2$, and $\bar{X} = f(X) = f_1 X \cup f_2 X$, then

$$f^{-1} \bar{X} = (X \cap D_1) \cup (X \cap D_2) = X \quad (3.1)$$

Hence, f^{-1} is defined at the image \bar{X} of f . Let us consider the preimages

$$f_i^{-1} d_{ijk}, \quad d_{ijk} = d_{ij} \cap D_k, \quad i, j, k = 1, 2, \quad (3.2)$$

Lemma 4.

- 1) The number of domains d_{ijk} is finite for $\mu > 0$ and countable for $\mu = 0$.
- 2) $\bigcup_{ijk} f_i^{-1} d_{ijk} = d_1 \cup d_2$.
- 3) $f_i^{-1} d_{ij1}$ and $f_i^{-1} d_{ij2}$ are narrow strips which intersect disk d_i and alternating in each region $d_i \cap D_k$, $i, j, k = 1, 2$.

The first assertion is true by virtue of the infinite (finite) numbers of points in the set $f_i l_{\xi}^i \cap C_0^1$ at $\mu = 0$ ($\mu > 0$); the other two assertions are obvious due to the inverse map f^{-1} .

We denote the domains $d_{ijk} = d_{ijkl}$ and $d_{ijkl}^{-1} = f_i^{-1} d_{ijkl}$, $i, j, k = 1, 2$, $l = 1, 2, \dots$, where l corresponds to the number of the domain intersections $d_{ijk} \cap \{\phi = 0, \phi = -\pi\}$ as $|x|$ decreases along the lines $l_0^{1(2)}$ and $l_{-\pi}^{1(2)}$. Denote also the intersections

$$V_L = d_{ijkl} \cap d_{i'j'k'l'}^{-1} \quad (3.3)$$

where L is the index vector with the coordinate values $i, j, k, i', j', k' = 1, 2$, $l, l' = 1, 2, \dots$. In view of the intersections in (3.3), new index in L appears which we will denote by $m = 0, 1, 2$, where "0" corresponds to one-component tangent intersections, whereas "1" and "2" correspond to left and right transversal intersections (see Fig.4).

Definition 2. Let X be a subset of D which is homeomorphic to a union of disks in \mathbb{R}^2 . We define a topological B -operator as the map

$$BX = (fX \cap X) \cup f^{-1}(fX \cap X) \quad (3.4)$$

Some properties of the B -operator are as follows.

1) $BX \subset X$. Indeed since $fX \cap X \subset fX$ and $fX \cap X \subset X$ it follows that $f^{-1}(fX \cap X) \subset X$ and $BX \subset X$.

2) If $fX \subset X$ then $B=f$ and $A=\lim_{p \rightarrow \infty} B^p D$ in view of (2.4).

3) If Ω_x is the limiting set of $f|_X$ such that $f\Omega_x = f^{-1}\Omega_x = \Omega_x$ then $B\Omega_x = \Omega_x$.

By virtue of these properties the B -operator allows us to determine any limiting set component as stable, unstable or hyperbolic. Moreover it is easy to verify that $\bigcup_L V_L = B(d_1 \cup d_2)$.

4. Limiting set.

Observe that the limiting set $\Omega = \lim_{p \rightarrow \infty} B^p(\bigcup_L V_L)$, i.e. the attractor A , is rather complicated because of the inevitable existence of the tangent components V_L ($m=0$) for which hyperbolicity does not hold [Gavrilov & Shil'nikov, 1972, 1973, Newhouse, 1979]. Let us divide the union $\bigcup_L V_L$ into two parts

$$\bigcup_L V_L = V^h \cup V^0$$

such that V^h (V^0) is the union of all transversal (tangent) intersections (3.3) for $m=1,2$ ($m=0$ respectively).

Theorem 1. The limiting set of $f|_{V^h}$ $\Omega_h = \lim_{p \rightarrow \infty} B^p V^h$ is a hyperbolic set conjugate to the topological Markov chain with an infinite (finite) number of symbols for $\mu=0$ ($\mu>0$ respectively).

Omitting the proof of this theorem and noting that Ω_h encloses the "twin" Smale's horseshoes (an infinite number for $\mu=0$), coupled to each other via their preimages, we identify our new geometric object as an **attribute of the double scroll attractor; namely the double horseshoe.**

By virtue of lemmas 1 and 2 for small μ and large l there exist two domains d_{211l_1} and d_{122l_2} such that the two intersections $V_{L_1} = (d_{211l_1} \cap d_{122l_2}^{-1})$ and

$V_{L_2} = (d_{122}l_2 \cap d_{211}l_1^{-1})$ in (3.3) are transversal (see Fig.5). We will henceforth call this combined geometric structure the double horseshoe. Here $\Omega(f|_{V_{L_1} \cup V_{L_2}}) = \lim_{P \rightarrow \infty} B^P(V_{L_1} \cup V_{L_2})$ is conjugate to the topological Markov chain with four symbols and characterized by the graph matrix

$$G = \begin{pmatrix} 0 & 0 & 1 & 1 \\ 0 & 0 & 1 & 1 \\ 1 & 1 & 0 & 0 \\ 1 & 1 & 0 & 0 \end{pmatrix}.$$

Moreover, one can verify the existence of fourfold, ..., 2^n -fold horseshoes with any mutual coupling among them.

In order to study the general case of Ω , and the special case $\Omega(f|_{V_0})$, note that for $\mu=0$ each "one-side" map $f_i: D_i \rightarrow D_i$, when restricted to the small half-neighborhoods $U_i \subset D_i$ of the homoclinic points P_i , $i=1,2$, is the subject of various theorems from [Ovsyannikov & Shil'nikov, 1986, 1991]. Their assertions applied to the map f are as follows.

Corollary. 1) For $1/2 < v < 1$ the set of parameters which implies the existence of structurally unstable periodic orbits, and a countable set of stable periodic orbits of each map $f_i|_{U_i}$, $i=1,2$ is dense.

2) For $v < 1/2$ the map $f_i|_{U_i}$, $i=1,2$ has no stable points.

Though this corollary isolates only a small subset of A in a small non-attracting vicinity of U_i , we obtain nevertheless an impressive information concerning the complexity of the trajectory behavior.

In the general case we need to study the feedback mapping $D_1 \rightarrow D_2 \rightarrow D_1$ and not for U_i only, but for the whole attracting regions d_1 and d_2 . But the most fundamental question in this study is: can attractor A be strange? The main result of this letter which we present in the next section, is that indeed A can be proved rigorously to be

a strange attractor.

5. Strange attractors.

First instead of the map f let us consider the map $F_k: \mathbb{R}^2 \rightarrow \mathbb{R}^2$ defined for each $k=0,1,2,\dots$ as follows:

$$\begin{aligned}\bar{x} &= \mu \operatorname{sgn} x - a|x|^v \sin(\phi + \phi - \omega \ln |x|), \\ \bar{\phi} &= -\pi/2 - \pi k + (\pi/2 + \pi k + a|x|^v \cos(\phi + \phi - \omega \ln |x|) \operatorname{sgn} x, \\ k &= 0, 1, 2, \dots\end{aligned}\tag{5.1}$$

Observe that $F_0=f$. For $k \geq 1$, F_k is a generalization of f , which need not be related to the PL-system. Obviously all previous results are still applicable for the case $k \geq 1$ with the only difference being that the distance between the centers of d_1 and d_2 is equal to $-\pi(2k+1)$.

Theorem 2. Assume

$$v < 1/2\tag{5.2}$$

then the map F_k for any $k=0,1,2,\dots$ has a strange attractor if

$$\frac{v(x_s - \mu)^2}{x_s} > 1\tag{5.3}$$

where x_s is the fixed point of (2.2), i.e. $x_s = \mu + ax_s^v$.

Proof. 1) F_k is an attracting map because

$$F_k(d_1 \cup d_2) \subset (d_1 \cup d_2), \quad k=0,1,2,\dots, \quad d_{1(2)} \subset \{ |x| \leq x_s \}$$

2) Consider the Jacobian matrix for F_k

$$DF_k = \begin{pmatrix} \bar{\phi} & \bar{\phi}_x \\ \bar{x} & \bar{x}_x \end{pmatrix}$$

and its determinant

$$\det DF_k = va^2 |x|^{2v-1} \quad (5.4)$$

For the region $\{|x| \leq x_s\} \supset (d_1 \cup d_2)$, i.e., for any $0 < q \leq 1$, $|x| = qx_s$

$\det(DF_k) = \frac{v(x_s - \mu)^2}{x_s q^{1-2v}} > 1$ under conditions (5.2) and (5.3). Hence the attractor

$A \subset \{|x| \leq x_s\}$ has no stable orbits thereby proving that it is strange.

Corollary. For $\mu > a(2a)^{1/(1-v)}$ we have $d_1 \subset \{x > 0\}$, and $d_2 \subset \{x < 0\}$. Hence $A = A_1 \cup A_2$, $A_i \subset d_i$, $i=1,2$ such that A_1 and A_2 are two separate non-interacting spiral-type strange attractors.

Remark. It follows from (5.2) and (5.3) that $ax_s^v > \pi/2$ and $f = F_0$ due to $d_1 \cap d_2 \neq \emptyset$ at $\mu = 0$ is no longer a one-to-one map. This constraint is the consequence of the condition (5.3) and the assumption that the map S is linear. Hence in order to avoid this constraint while preserving (5.3) we need to consider the nonlinear case of S .

Consider now again the map f in the case

$$\sqrt{(2\mu)^2 + \pi^2} > 2(x_s - \mu) \quad (5.5)$$

where it still corresponds to the PL-system, because $d_1 \cap d_2 = \emptyset$ in view of (5.5).

Theorem 3. For small values of $\delta_1 > 0$ and parameters of f from the "resonance zones" defined by

$$\Delta_1 = |\varphi - \omega \ln x_s - (\pi/2)(2n+1)| < \delta_1, \quad n \in \mathbb{Z} \quad (5.6)$$

the attractor A has stable periodic orbits and is therefore *not strange* under the condition

$$x_s - \mu < 1, v < 1 \quad (5.7)$$

for any $\mu \geq 0$ in the case of "even" n , and for some small $\mu \geq 0$ in the case of "odd" n .

Proof. One can immediately verify that for $\Delta_1 = 0$ and for "even" n 's $f_{1(2)} M_{1(2)} = M_{1(2)}(M_1(0, x_s), M_2(-\pi, -x_s))$ and the multipliers for those points $s_1 = x_s - \mu < 1, s_2 = v(1 - \mu/x_s) < 1$ in view of (5.7). Therefore $M_{1(2)}$ is a stable fixed point for any μ . Moreover for $\Delta_1 = \mu = 0$ and for "even" n 's, the map f has two stable periodic orbits $N_1 = f_2 N_2$ and $N_2 = f_1 N_1$ ($N_1(-\pi, x_s), N_2(0, -x_s)$); and for "odd" n 's f has a stable 4-periodic orbit $M_1 \rightarrow N_2 \rightarrow M_2 \rightarrow N_1 \rightarrow M_1$. Hence small changes in Δ and μ can not destabilize the stable points. This proves the theorem's assertion.

Theorem 4. Assume that for small $\delta_2 > 0$ the condition

$$\Delta_2 = |\varphi - \omega \ln x_s - \pi n| < \delta_2, n \in \mathbb{Z} \quad (5.8)$$

holds. If

$$v(x_s - \mu)^2/x_s > q_m^{1-2v}, \quad v < 1/2, \quad (5.9)$$

where

$$q_m = \frac{1}{x_s} \left(\mu + \Delta x + \frac{\omega \alpha x_s^v}{\sqrt{v^2 + \omega^2}} \exp\left(-\frac{v}{\omega} \arctan \frac{\omega}{v}\right) \right) < 1 \quad (5.10)$$

then the attractor A is *strange*.

Proof. In the case of $\Delta_2 = 0$ (unlike $\Delta_1 = 0$) the image of the boundary points $M_{1(2)}$ lies at $\{|x| = \mu\}$. Hence, the second image $d_{ij} \subset \{|x| \leq x_m\}$, where $x_m < x_s$ is the maximum value of $|x|$ for $d_{ij}, i, j = 1, 2$. Hence a sufficient condition for the attractor A to be strange is

$$\det Df|_{x=x_m} = \frac{v(x_s - \mu)^2}{x_s} \left(\frac{x_m}{x_s} \right)^{2v-1} > 1, \quad v < 1/2 \quad (5.11)$$

In order to obtain a rough approximation of x_m let us put $n=0$ in $\Delta_2=0$ and pick the maximum of the image f_1^1 , which is the middle line of d_{12} , and has the following parametric equations:

$$\bar{\phi}(x) = -ax^v \cos(\varphi - \omega \ln x), \quad \bar{x}(x) = \mu + ax^v \sin(\varphi - \omega \ln x), \quad x \in (0, x_s], \quad (5.12)$$

Substituting in (5.12) the largest solution x_0 of the equation $\bar{x}'_x = 0$, which is equal to $\text{Sup}_x(\bar{x}(x))$, and adding it to some value $\Delta x > 0$ to compensate the width of the S-snake d_{12} , we obtain the value $x_m = q_m x_s$, where q_m is defined by (5.10), $q_m < 1$. Substituting x_m in (5.11) we obtain the condition (5.9) for the attractor A to be strange.

Consider $\delta_2 > 0$ in (5.8) such that $M_{11} \in \{|x| < x_m\}$ and so condition (5.11) is still true for $x_m = q_m s$. Hence the attractor A is strange under the conditions of the theorem.

Figure 6 shows only one trajectory of the map f inside of the region $d_1 \cup d_2$ for some values of the parameters corresponding to the strange attractor.

Conclusions.

We have presented a new type of strange attractor which gives rise to a new point of view on the original geometry of the double scroll family generated by Chua's circuit.

Our current attractor is much more complicated than the Lorenz-type attractor [Afraimovich et.al. 1983]. Although the above model represents the simplest

idealization of the double scroll attractor we hope that the main features of this attractor will be preserved in the general nonlinear case. For example, the case

$$SY = S_0 + S_1 Y + \frac{1}{2} Y^T S_2 Y + \dots$$

represents an important basic problem for future investigation.

References

- Afraimovich, V.S., Bykov, V.V., Shil'nikov, L.P. [1983] "On structurally stable attracting limit sets of the Lorenz attractor type", *Trans. Moscow Math. Soc.* 1983, Issue 2, 153-216.
- Chua, L.O., Komuro, M. & Matsumoto, T. [1986] "The double scroll family, Part I and Part II", *IEEE Trans. Circuits and Systems CAS-33*, 1072-1118.
- Gavrilov, N.K., Shil'nikov, L.P. [1973] "On three dimensional dynamical systems close to systems with a structurally stable homoclinic curve", *Math. USSR Sb.* v.19, 139-156.
- Komuro, M., Tokunaga, R., Matsumoto, T., Chua, L.O., Hotta, A. [1991] "Global bifurcation analysis of the double scroll circuit", *Int. J. Bifurcation and Chaos* 1(1), 139-182.
- Matsumoto, T. [1984] "A chaotic attractor from Chua's circuit", *IEEE Trans. Circuits and Systems*, v.31(12), 1055-1058.
- Newhouse, S.E. [1972] "The abundance of wild hyperbolic sets and non-smooth stable sets for diffeomorphisms", *Publ. Math. IHES*, 50, 101-151.
- Ovsyannikov, I.M. and Shil'nikov, L.P. [1986] "On systems with a homoclinic curve of the saddle-focus", *Matem. Sbornik*, v.130(172), 552-570 (in Russian).
- Ovsyannikov, I.M. and Shil'nikov, L.P. [1991] "Systems with homoclinic curve of the multi-dimensional saddle-focus and spiral chaos" *Matem. Sbornik*, v.182, #7, 1043-1073 (in Russian).
- Shil'nikov, L.P. [1965] "A case of the existence of a denumerable set of periodic motions", *Sov. Math. Dokl.* 6, 163-166.

Figure captions

Fig.1. Global geometric model of the PL-system showing two odd-symmetric homoclinic orbits through the origin and their tubular neighborhood for flows under the linear map (1.4). The return points P_1 and P_2 are drawn for the case $\mu = 0$. For the general case $\mu > 0$, the center P_1 (P_2) of the right (left) circle is translated upward (downward) by an amount equal to μ .

Fig.2. By cutting the cylinder surface D vertically at $\phi=\pi/2$ and identifying the two vertical boundaries, we obtain the equivalent planar representation of the unwrapped cylinder. Each arrow denotes the mapping from the indicated line segment to either a circle or a spiral. In particular, each horizontal line C_η^1 (C_η^2) located at $x = \eta$ on the upper half (lower half) rectangle D_1 (D_2) maps into a circle; each vertical line segment l_ξ^1 (l_ξ^2) on the upper half (lower half) rectangle D_1 (D_2) maps into a spiral.

Fig.3. The image of the upper or lower half portion of the disks d_1 and d_2 gives rise to 4 Shil'nikov snakes: $d_{11} = f_1(D_1 \cap d_1)$, $d_{21} = f_2(D_2 \cap d_1)$, $d_{12} = f_1(D_1 \cap d_2)$, $d_{22} = f_2(D_2 \cap d_2)$.

Fig.4. Each shaded region denotes the intersection between the image and the preimage of one Shil'nikov snake.

Fig.5. Schematic diagram showing the double horseshoes resulting from the map defined by the geometric model.

Fig.6. (a) A typical strange attractor of the spiral (Rossler) type generated by the geometric model for the indicated parameters values.

(b) A typical strange attractor of the double scroll type generated by the geometric model for the indicated parameters values.

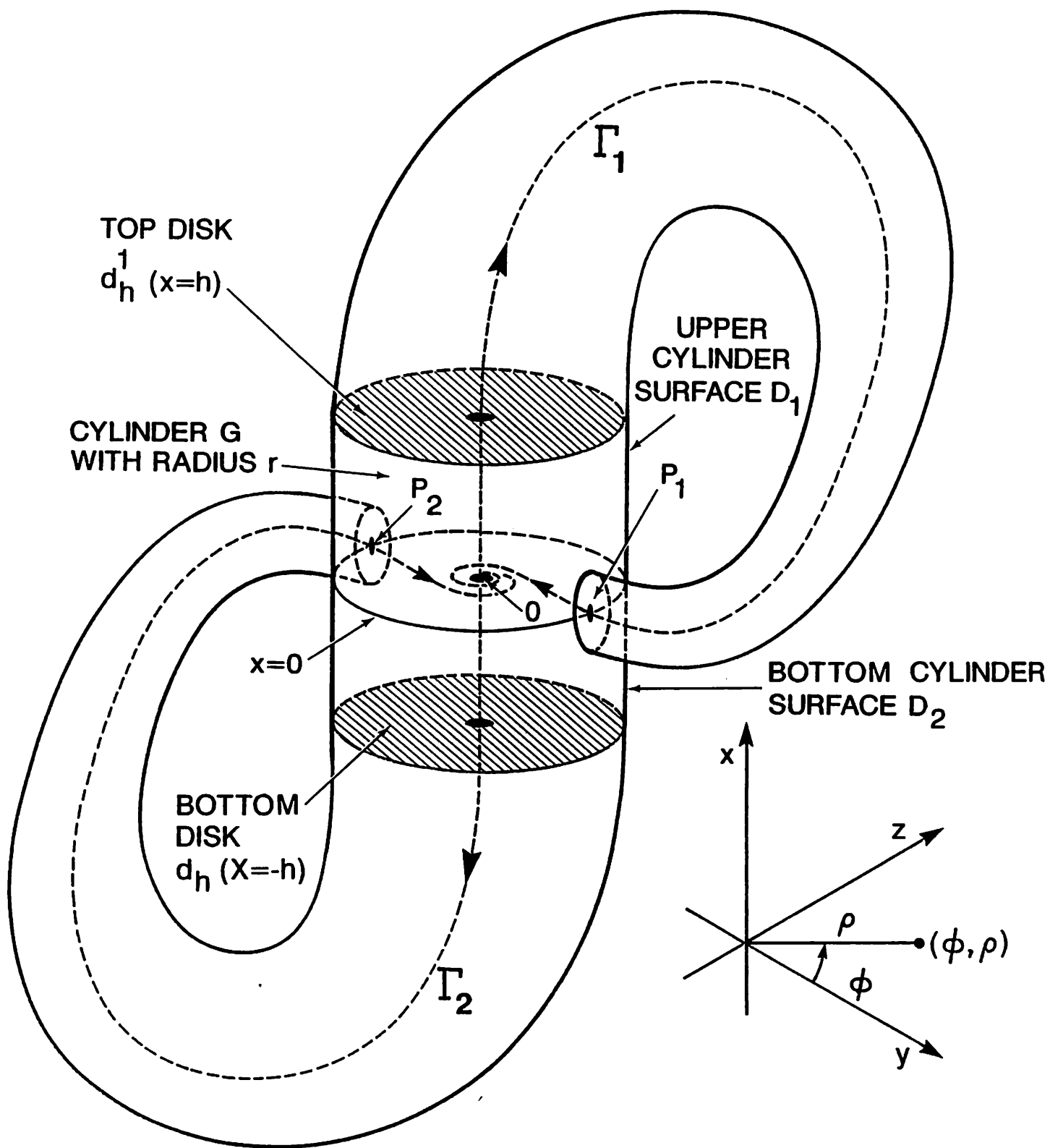


Figure: 1

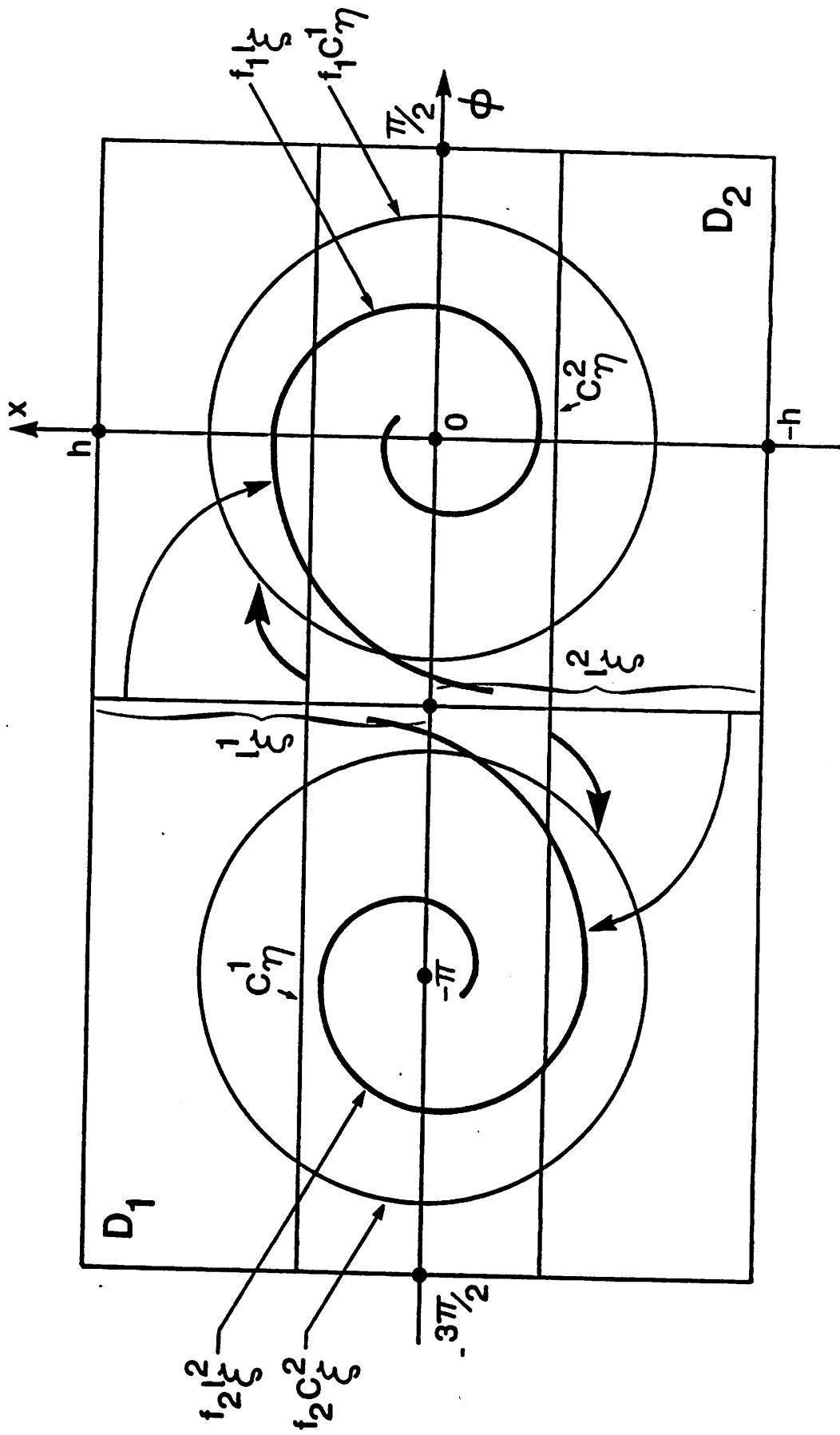


Figure: 2

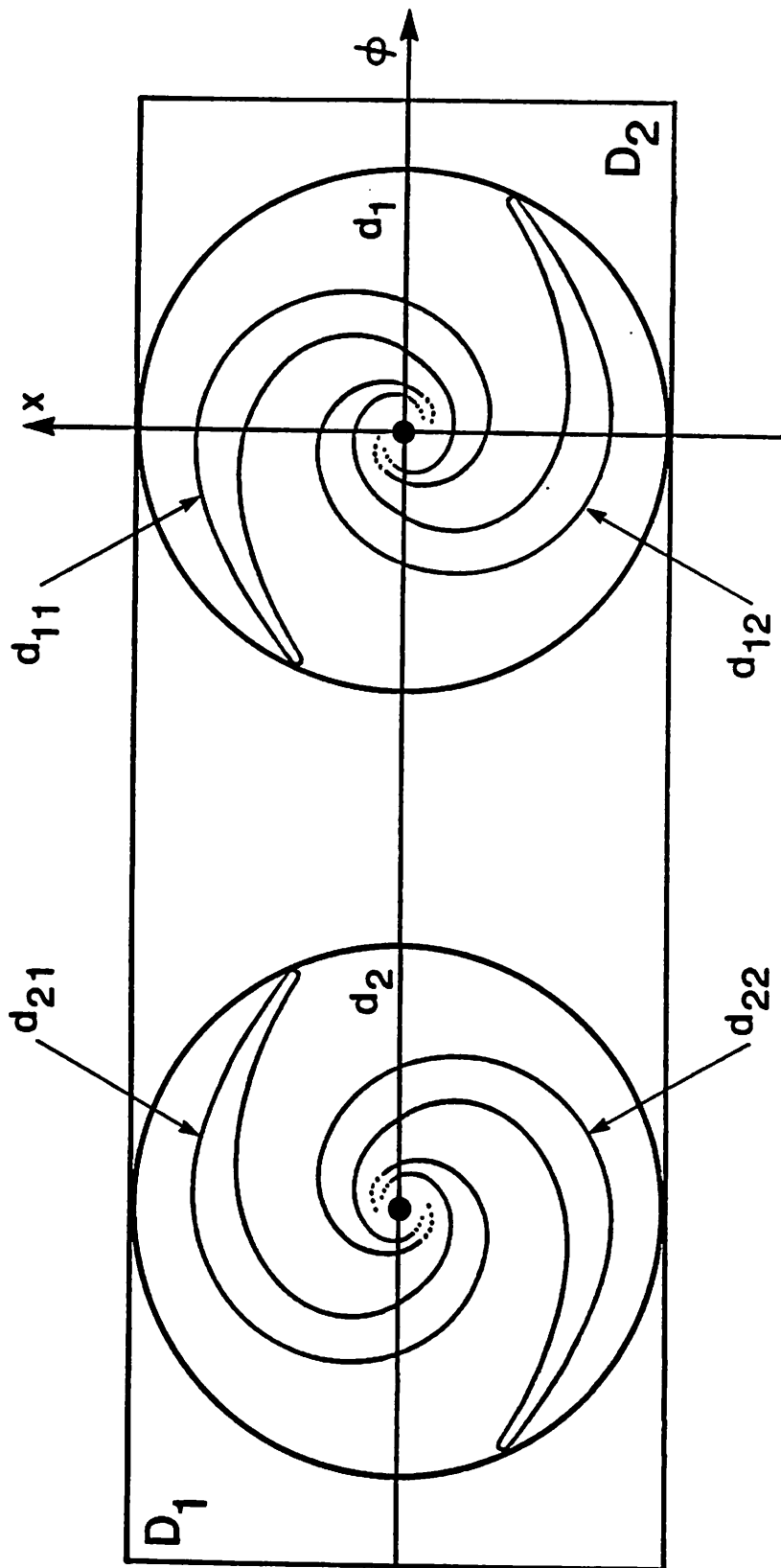


Figure: 3

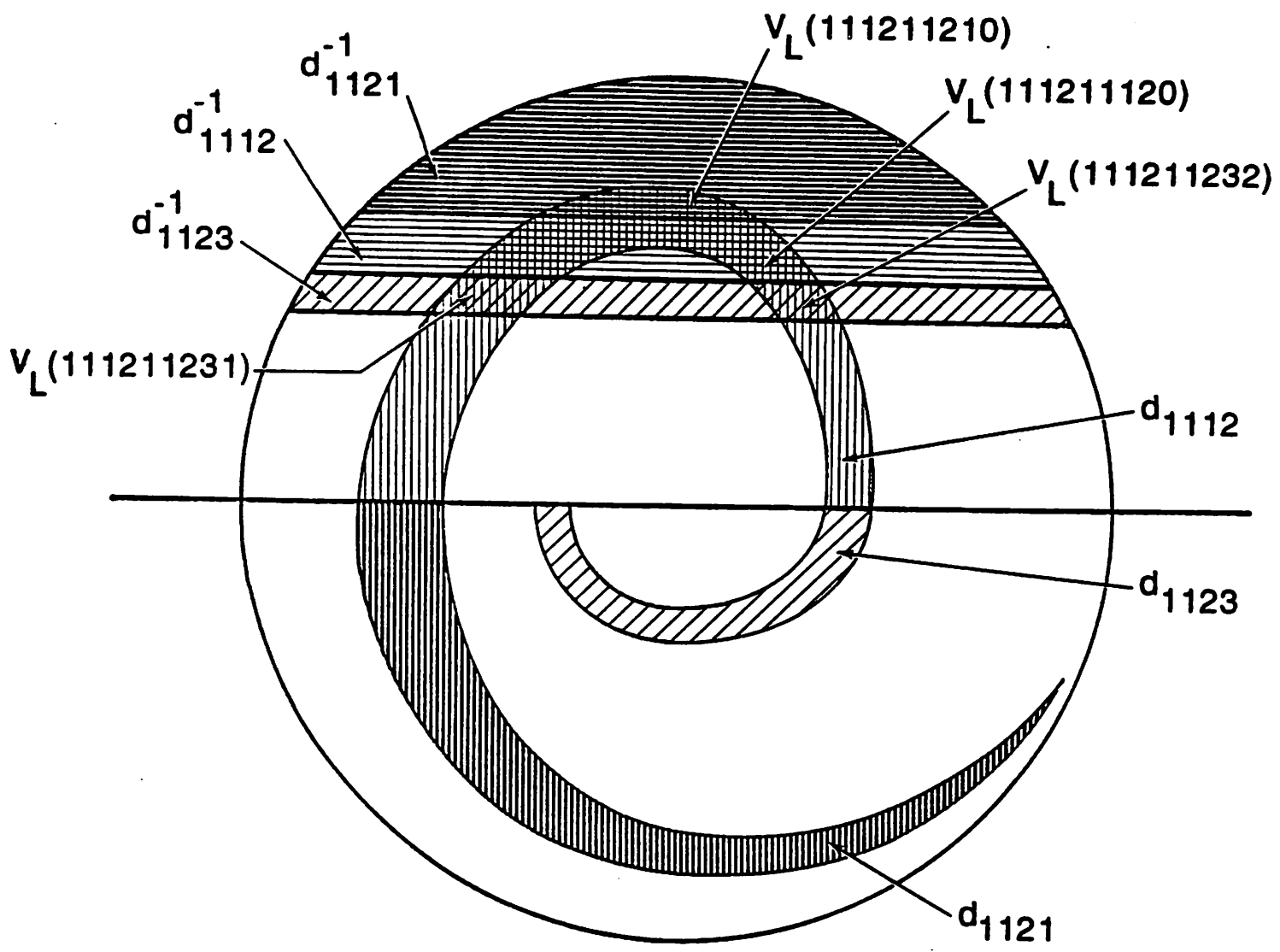


Figure: 4

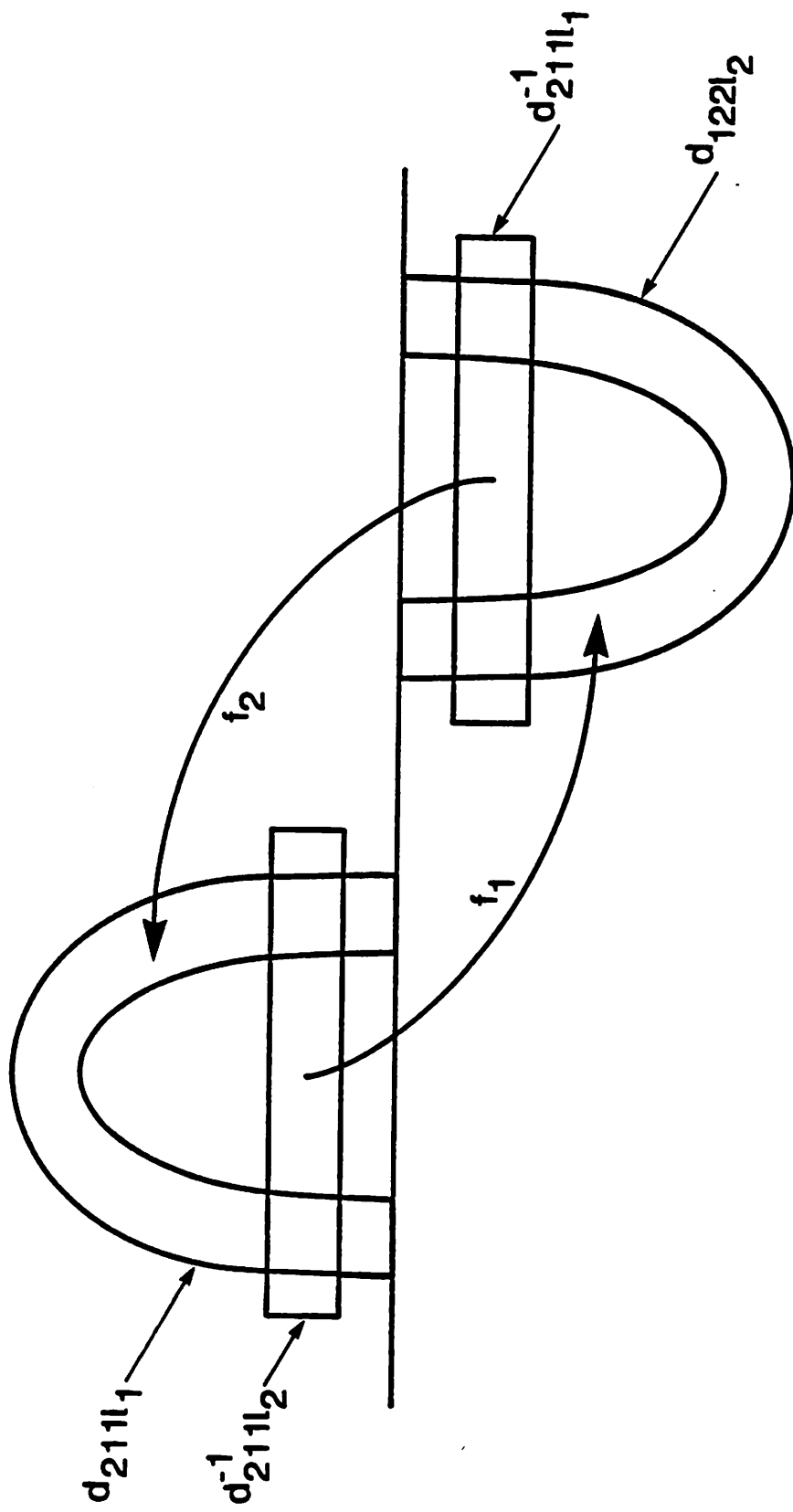


Figure: 5

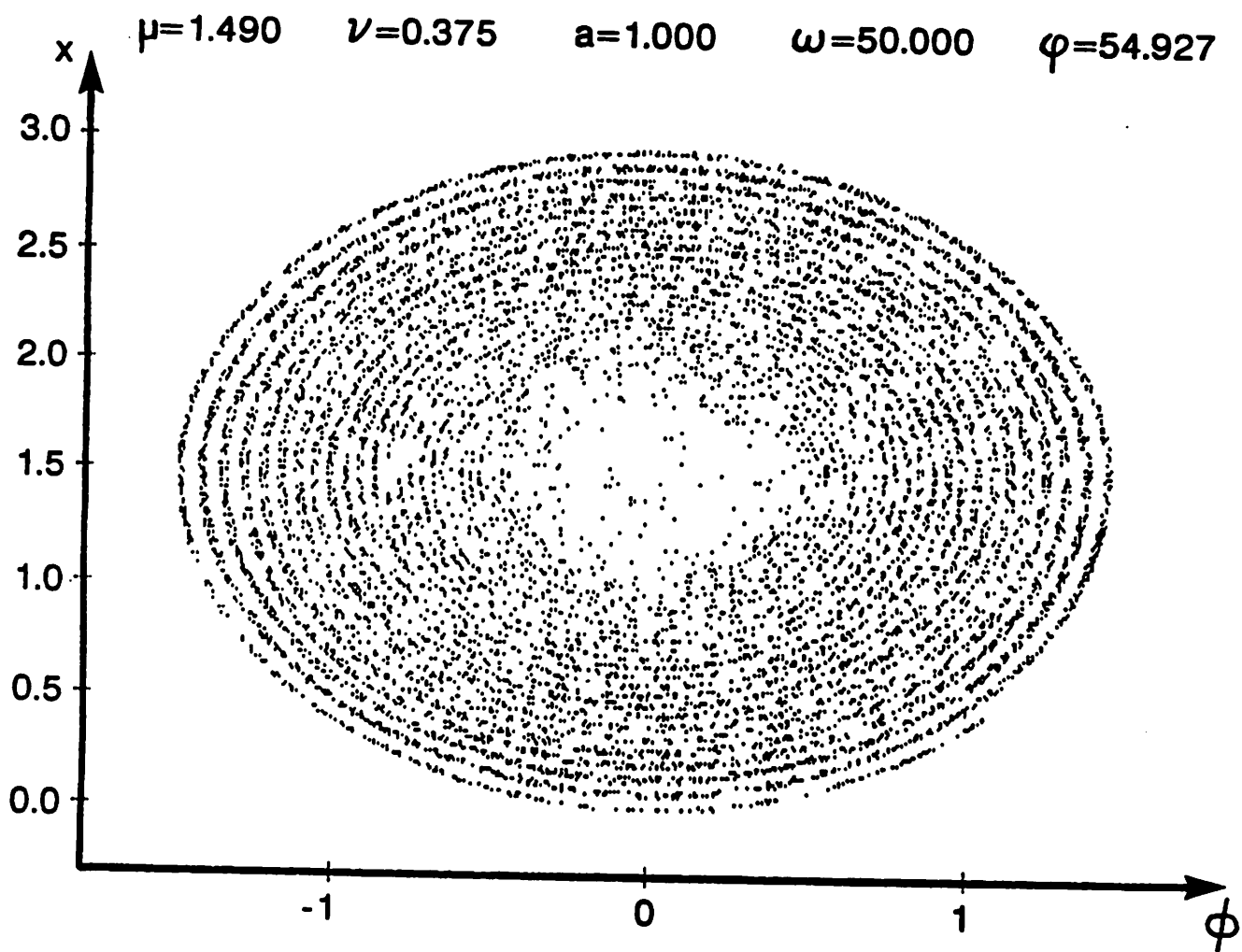


Figure: 6 (a)

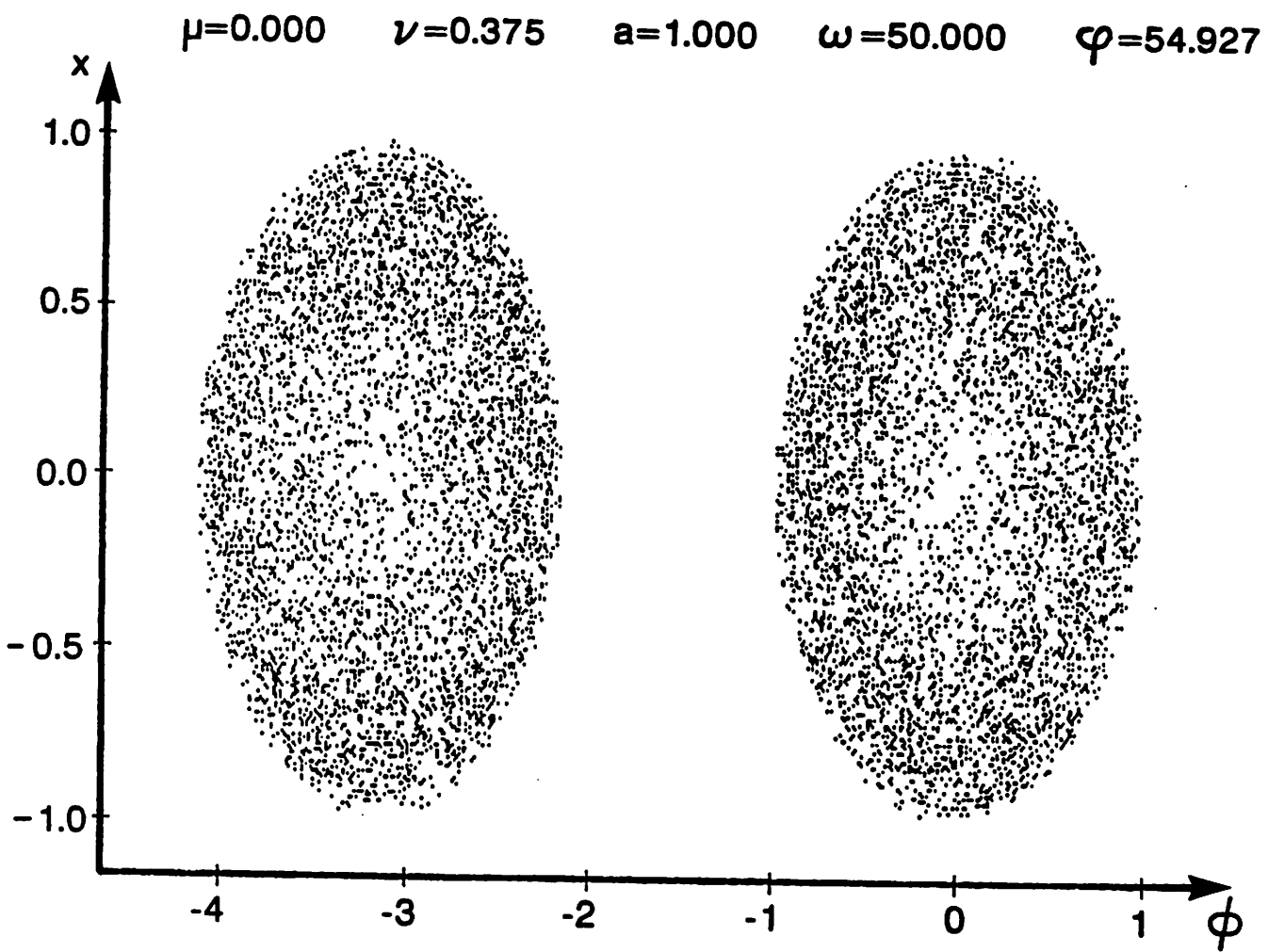


Figure: 6 (b)